Progress In Electromagnetics Research B, Vol. 90, 43–62, 2021

Design of a Controllable Antenna Based on Embedded Differential PSK Modulation

Yahiea Alnaiemy[1, 2, *] and Lajos Nagy[1]

Abstract—Direct Antenna Modulation (DAM) is explored recently in many wireless communication systems. In this paper, we explore the modulation process of electromagnetic signals in the antenna circuit design directly. The proposed antenna consists of two non-concentric elliptical patches for broadband applications to suit the spread spectrum applications. To perform a Differential Phase Shift Keying (DPSK) modulation, two identical antennas are fed by a two-branch microstrip line with a phase shift. Utilizing Computer Simulation Technology of Microwave Studio (CSTMWS) based on Finite Integral Technique (FIT), an optimization based-on numerical analysis is adopted for designing the transmission line configuration at the desired frequency bands. The other significant aspect that has been achieved in this research is reducing the patch size to be suitable for wearable devices. Therefore, a cylindrical substrate is utilized for bending the proposed antenna structure. The proposed antenna design shows a gain of 4.73 dBi and 2.5 dBi for the planar and folded antenna profile, respectively. Two high-speed Positive Intrinsic Negative (PIN) diodes as switching elements of the RF signal are inserted between the identical antenna elements through a transmission line. Switch 1 (SW1) and switch 2 (SW2) are used to control the phase shift between the antenna elements by changing the switching state from (OFF-ON) and vice versa. The designed antenna is further investigated to realize the effects of radiation leakage from the antenna elements on the human body in the context of wearable applications. This study is conducted to the antenna performance when it is bent on a cylinder and compared to the flat case on four human body regions: arm, head, thigh, and chest. The proposed antenna based on PIN diodes is fabricated, measured, and tested. Using a 3D axis field strength meter, the proposed antenna system field strength is measured for different conditions at various locations of the human body. Finally, an excellent agreement is found between the obtained numerical results and measurements.

1. INTRODUCTION

Due to the rapid developments in present wireless communication and information technologies, several approaches have been developed based on Direct Antenna Modulation (DAM) process as alternatives to the classical modulation approaches [1]. DAM can be used to overcome the challenges based on modulation systems, such as high-cost, high-complexity transmitter design, which are inevitable in such modulation systems. Therefore, DAM has emerged as a practical approach to overcome drawbacks of such modulation systems [2]. DAM's principal idea is to allow modulation of the carrier wave in the antenna structure [3]. Based on an array of switchable passive reflectors for reconfigurable antennas, different DAM approaches were suggested [4]. These developments add more capabilities to resolve the complexity relative to the development of such wireless communications [5]. Unlike conventional electromagnetic devices such as antennas, artificial or smart antennas can be produced

Received 1 October 2020, Accepted 18 December 2020, Scheduled 29 December 2020
* Corresponding author: Yahiea Alnaiemy (yahiea@hvt.bme.hu).
[1] Department of Broadband Infocommunications and Electromagnetic Theory, Faculty of Electrical Engineering and Informatics, Budapest University of Technology and Economics, Budapest, Hungary. [2] Department of Computer Science, College of Science, University of Diyala, Iraq.

renewable and from local non-conventional devices that are well matched with the rapid developments in communication and information technologies [6]. Moreover, combining the reconfigurable antenna with other communication devices in the engineering electromagnetic applications to produce new electromagnetic devices is a versatile and reliable solution of development, enabling the antennas, wireless sensors, solar cells, smart clothes, and wearable microwave devises [7]. The intimate relationship between the new technologies and communication developments is through finding methods to satisfy the requirements of these developments that can substitute the traditional approaches [8]. Transitional technologies to merge between the antenna designs and semiconductors helped the rapid growth in wireless communication markets; however, this merge still requires novel antennas to find alternative solutions for many obstacles, including the design complexity and size reduction [9]. Therefore, the present wireless communication technology invoked tremendous interest in smart antennas, especially for 4G and 5G [10]. For this, the researchers have been attracted to utilize reconfigurable smart antennas to improve the wireless communication systems performance in different applications [11–13]. However, they faced a new challenge: integrating antennas with modern high-speed semiconductors while maintaining the size miniaturization and keeping high gain-bandwidth produce over the frequency band of interest [14, 15]. Based on such techniques, several trades-offs are among the antenna characteristics such as antenna size, antenna geometry, and effects of these parameters on the antenna design performances [15]. Therefore, the main key design is focused on the antenna characteristics isolation from the high-speed semiconductor switching devices in the communication system [16]. Many researchers utilized different RF switches such as MEMS, varactor diodes, transistor switches, and PIN diodes for current and future wireless communication systems by enabling frequency, pattern, and polarization reconfigurability [17–45]. Reconfigurable antennas based on polarization, radiation patterns, and frequency are reported in [17–45] by integrating PIN diodes, RF MEMS, and varactor diode into a device platform as switches to control the polarization, radiation direction, and frequency operation bands. The PIN diodes are considered one of the most important Radio Frequency (RF) switches due to their high-speed response and low forward resistance with low capacitance [17]. For example, PIN diodes as switches on a monopole antenna were proposed for frequency reconfiguration in [18]. An antenna of circularly polarized structure based on an Electromagnetic Band Gap (EBG) array was proposed for frequency and polarization reconfiguration techniques as presented in [19]. For frequency and polarization reconfiguration, an antenna design based on single PIN diode integrated to a folded slot patch on a flexible substrate was discussed in [20]. The proposed antenna in [21] was designed to work on the 2.45 GHz frequency band when the PIN diode was set to ON state while it worked at 2.36 GHz and 3.64 GHz, when the diode was switched to OFF, making the proposed antenna design suitable for the WLAN and WiMAX applications. The developed antenna in [22] was designed with two PIN diodes as switching circuits to directly control two binary Phase Shift Keying (PSK) modulated signals. A reconfigurable aperture antenna design was discussed in [23]; the reconfiguration was utilized based on using Field Effect Transistor (FET) switch to meet different antenna performances; however, the design was quite complex and large. For time delay beam steering in an ultra-wideband (UWB) antenna array, the authors in [24] proposed a complementary metal-oxide-semiconductor (CMOS) technology for the beam steering process. The authors in [25] designed an array of 7×7 patch elements for beam steering based on tunable functions. Integrating three Schottky diodes (HSCH-5330) as switching devices on the slots for DAM was presented in [26] for the UWB transmitting antenna design. A switchable band notch based on PIN diode integrated with Complementary Split Ring Resonators (CSRR) slot for reconfigurable monopole UWB antenna was investigated in [27] underlay cognitive radio applications. Single and dual stopbands for a printed UWB slot antenna were presented in [28] by using two PIN diodes embedded across the circular slot patch antenna to suit the WiMAX and WLAN bands. Three PIN diodes were utilized in [29] for a reconfigurable filter antenna to suit the impulse radio UWB, WLAN, and WiMAX applications. Changing between frequency and pattern reconfigurability was achieved in [30] based on three PIN diodes switches. By adjusting the three PIN diodes state (ON-OFF) and depending on the switch, the condition can easily convert the antenna reconfigurability between the frequency and beam directions. In UWB, WiMAX and WLAN rejection bands were controlled based on two PIN diodes using an open-ended slot and a U-shaped slot for the modified monopole antenna [31, 32]. Two orthogonal antennas were introduced in [33] to realize a circularly polarized Quadrature PSK (QPSK) modulated signal. A switchable Frequency Selective

Surface (FSS) based on ASK modulator was described in [34] for the THz communication application. Radio frequency carrier DAM was discussed in [35] as a phase modulator for the Internet of Things (IoT) applications based on reconfigurable FSS. A DAM On-Off Keyed (OOK) signal based narrowband transmitter antenna was studied in [36] for inter-symbol interference. 8-PSK modulation with 8×32 phase unit cells was demonstrated in [37] of a transmitter based on programmable metasurface. In Ka-band, a linearly polarized reconfigurable, beam-steering antenna with a 2-bit phase resolution was presented in [38]. The authors in [38] utilized transmission phase to control four PIN diodes switching on the radiating patches based on six metal layers of dielectric and film substrates.

In this article, a novel technique for embodying the electromagnetic signal modulation in antenna circuitry is investigated. Therefore, the antenna structure is designed based on integrating high-speed circuits of two PIN diodes. The modulation technique is optimized at the resonance frequency by modulating the carrier wave signal directly in the antenna structure with a semiconductor switching device that controls the baseband information signal phase change, encoded into a digital pulse stream. The pulse train controls the antenna phase shift and modulates the transmitted carrier wave effectively by biasing the semiconductor switch. Simultaneously, the antenna is designed to operate at broad bandwidth to be ideal for spread spectrum applications achieved by partial ground plane structure. Another significant achievement in this work is the antenna structure miniaturization to make the antenna suitable for biomedical devices. The use of a traditional impedance-matching network with different lengths to realize the phase shift between antennas is proposed. The proposed network is based on two lines with two different lengths (l_2 and l_1) to provide a phase shift of 180° as seen in Equation (1):

$$(\Delta l)\beta = (l_2 - l_1)\frac{2\pi f}{vp} = 180^\circ \tag{1}$$

where Δl is the difference between the physical lengths, β the phase propagation constant, f the frequency band of interest, and v_p the phase velocity.

Therefore, two RF PIN diodes are the key elements of the proposed reconfigurable design; the phase shift between two identical slotted patch elliptical antennas is controlled through two switches, (SW1 and SW2). By adjusting the switch states via the voltage biasing of the PIN diodes, which are positioned between slotted patch elliptical antennas, a phase shift with 180° is obtained by controlling the current to pass through the transmission line with different lengths. The numerical simulations using CSTMW based on FIT are performed to examine the proposed antenna properties. This paper is organized as follows. In Section 2, the proposed design aims is introduced. Design planar and folded antenna profile is described and discussed in Section 3. In Section 4, the proposed antenna performances with planar and folded profiles are discussed. The results validation and measurements are presented and compared in Section 5. In Section 6, antenna performance-based wearable applications are explored. Finally, the paper is concluded in Section 7.

2. DESIGN METHODOLOGY

Design of the microstrip patch antenna for wearable biomedical applications based on a modulation circuitry system is investigated in this section. The patch antenna structure based on a single microstrip antenna is centered on a slotted patch elliptical structure. The slotted patch structure is investigated to increase the proposed antenna bandwidth to be a good candidate for spread spectrum systems. Therefore, to apply the antenna for wearable applications, the proposed antenna structure is placed on a flexible substrate. Nonetheless, a pair of the same antenna structure is aligned with each other for DPSK modulation. The patch structure is fed with a $50\,\Omega$ microstrip line network of two branches, and one of them is delayed with 180°. Two BAR63-03W-SOD323 PIN diodes are utilized in this paper with high-speed RF switching signals. The main reason for choosing such type of PIN diodes is its high-speed switching, low forward resistance, and low capacitance [19]. The property of the PIN diodes acts as the forward resistance Rs in series and shunt capacitance with substantial resistance Rp for the two PIN diodes states ON and OFF, respectively [19], as indicated in Fig. 1.

The mean reason for utilizing such modulation is that it is possible to change the modulated signal phase relative to the previous signal. The DPSK reference signal, therefore, does not require an oscillator for comparison [37]. Fig. 2 describe the block diagram of the DPSK and the model waveform.

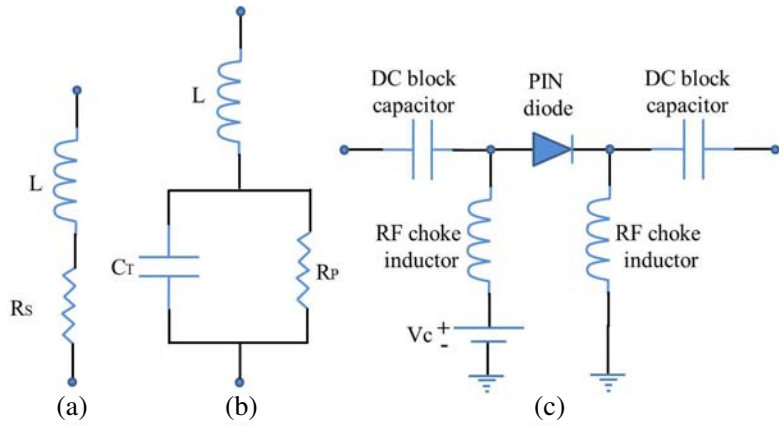

Figure 1. Equivalent circuit and configuration of the PIN diode bias circuit. (a) Forward bias, (b) reverse bias, and (c) bias circuit.

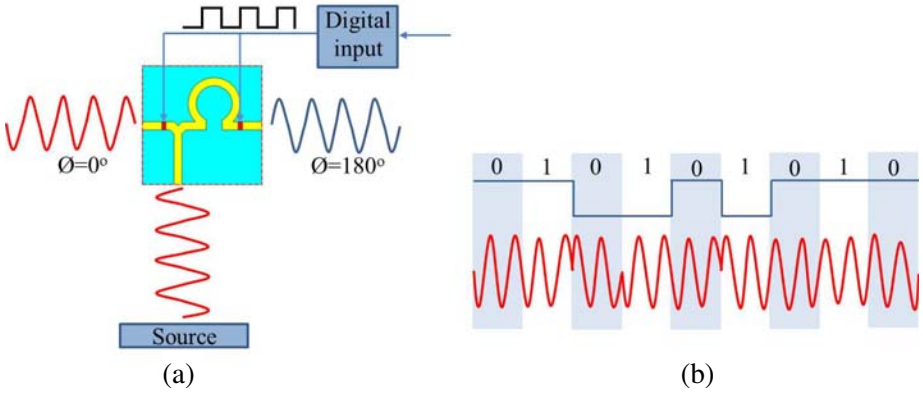

Figure 2. (a) The proposed method for achieving DPSK modulation using PIN diodes as switchable and (b) waveform of DPSK.

3. ANTENNA DESIGN

The proposed antenna structure is simulated numerically in both planar and folded profiles. The patch and ground plane are fabricated from copper and mounted on a lossy dielectric Roger RO3203 substrate with $\epsilon_r = 3.02$, and $\tan\delta = 0.0016$ of 1 mm thickness. The patch is formed as an elliptical slotted patch to enhance the antenna bandwidth to provide capacitive coupling inductions for the proposed antenna bandwidth enhancement [39].

3.1. Planar Antenna Profile

The proposed planar antenna profile is based on two identical slotted patch elliptical structures as depicted in Fig. 3. In this section, the authors utilize a single patch structure centered on the proposed antenna flat profile as a reference design to be adapted later to the folded configuration. Nevertheless, the antenna geometry characteristics are optimized to reach the optimal bandwidth as a single element. The authors targeted their work to achieve the modulation using a two-antenna array instead of a single antenna with two input ports. The main reason for using two antennas the degree of freedom is that the switching does not affect current distribution and radiation pattern. Therefore, this is considered to avoid the raise time delay required by the antenna switching process that could affect the modulation speed processing. Also, using a single antenna with two input ports may affect the antenna polarization severally. Therefore, we attempted this work to avoid affecting the antenna polarization. For only a

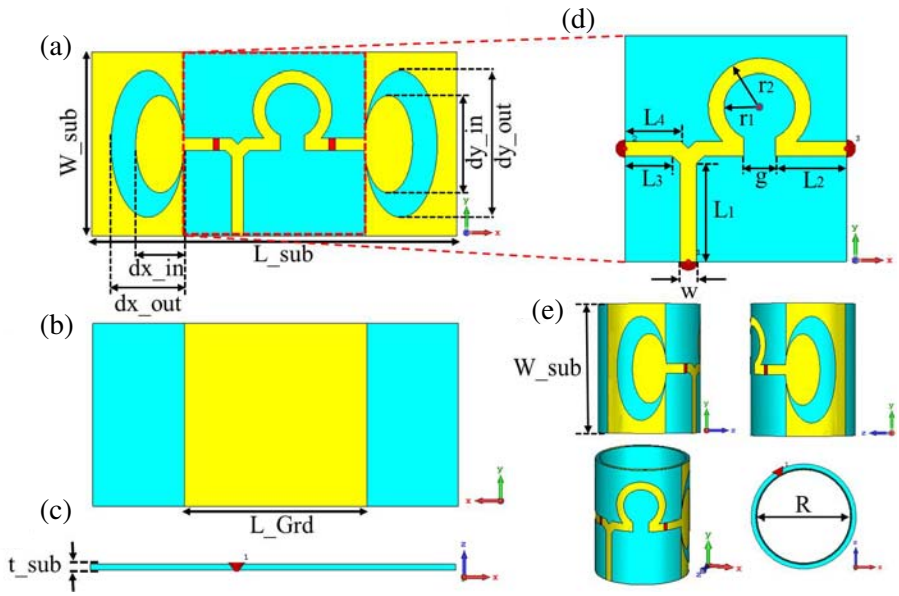

Figure 3. The geometrical antenna details; (a) front view, (b) backed view, (c) side view, (d) transmission line, and (e) cylindrical profile.

simulation process, a rectangular slot (SW1 and SW2) with 1 mm × 2 mm dimension is embedded and installed within the proposed antenna structure to connect the transmission line with the two slotted patches elliptical structure as shown in Fig. 3. Numerically, ON-OFF states of the PIN diodes are simulated with changing the short line material from Vacuum-to-PEC when changing the PIN states from OFF-to-ON and vice versa. A 50 Ω SMA connector is used to connect the antenna element to the RF source. Table 1 shows the geometrical dimension of the proposed antenna.

Table 1. Geometrical dimensions (mm) of the proposed antenna.

Parameter	Dimension	Parameter	Dimension	Parameter	Dimension
L_1	13	g	4	R	19
L_2	9.8	W	2	dy_out	24
L_3	6.8	W_sub	30	dy_in	16
L_4	7.8	L_sub	60	dx_out	12
r_1	4.5	t_sub	1	dx_in	8
r_2	6.5	L_Grd	30	-	-

3.2. Transmission Line Feed Network Structure

The transmission line network is designed to switch the feeding between the patches with a phase shift of 180° at the frequency band of interest. The switching mechanism is conducted using two PIN diodes, which are controlled by the base data signal as; if the bit value is one, then SW1 is ON, and SW2 is OFF; if the bit value is 0, then SW1 is OFF, and SW2 is ON. For wearable applications, the proposed antenna structure based on two antenna patches is folded on a flexible cylindrical substrate with a radius of 9.5 mm, as shown in Fig. 3.

4. RESULTS AND DISCUSSION

In this section, the planar and folded antenna profiles are performed for simulation in CST MWS based on FIT. The proposed antenna performance is evaluated in terms of the scattering coefficients, bandwidth, and radiation patterns. In this section, the design approach is applied to optimize the proposed antenna performance. The patch dimensions and feed length are adjusted concerning simulations through several iterative simulation steps to achieve an optimal phase shift across multiple bands. This approach is justified, as it is found that the resonant frequencies do not change significantly with a single antenna function observed performance. The simulations are conducted using CST MWS by running two tests: the first is sufficiently distinct by ensuring the geometry and fields. Perfectly Matched Layer (PML) is invoked at standard incidence with the reflection coefficient of 0.0001. The tetrahedral mesh is applied, and the second test is taken into account by setting the −80 dB accuracy limit.

4.1. Antenna Performance Based on Planar Profile

The numerical results indicate different resonance frequencies, but the authors concentrated on the frequency resonance on 5 GHz to match the current wireless communication systems and find similar impedance $|S_{11}| \leq -10$ dB for both cases, as shown in Fig. 4. The authors targeted, in their work, 5 GHz, because the phase shift between the two antennas is found to be 180°. Therefore, it is very wise to realize the antenna design at 5 GHz since the proposed transmission network shows a phase shift of 180° at this frequency.

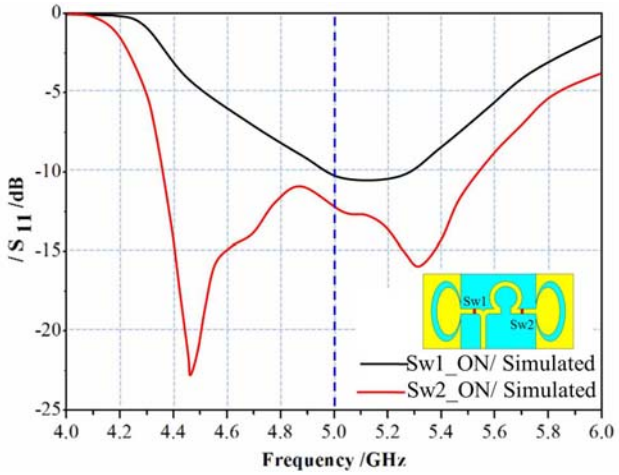

Figure 4. S_{11} Spectra of the proposed antenna at two switch cases based on planar profile.

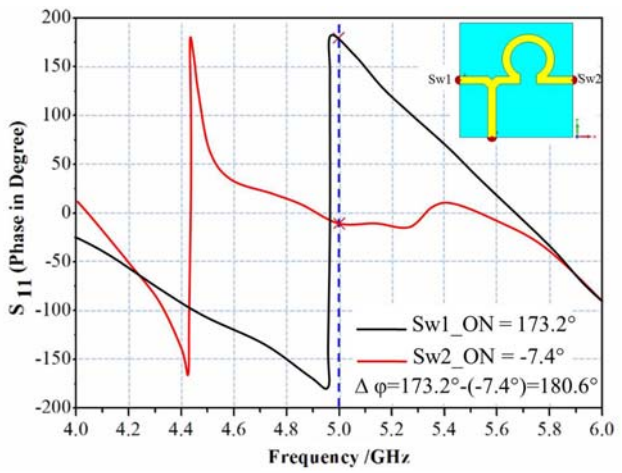

Figure 5. Phase difference spectra of the two switches cases.

4.2. Transmission Line Feed Network Structure

The authors have carried out numerical simulations to check the proposed transmission line network performance. S_{11} spectra of the proposed transmission line network are shown in Fig. 5. The numerical simulation results are conducted to test the transmission line network performance. The phase difference S-parameters of the proposed transmission line network are evaluated in Fig. 5 for both switch cases. It is indicated that a 180° phase difference is obtained at 5 GHz when the switches are changed (ON-OFF) and vice versa.

4.3. Antenna Performance Based on Folded Profile

A matching circuit with the best possible phase difference is performed to suit and achieve excellent matching at 5 GHz to preserve the proposed antenna performance after bending the proposed antenna

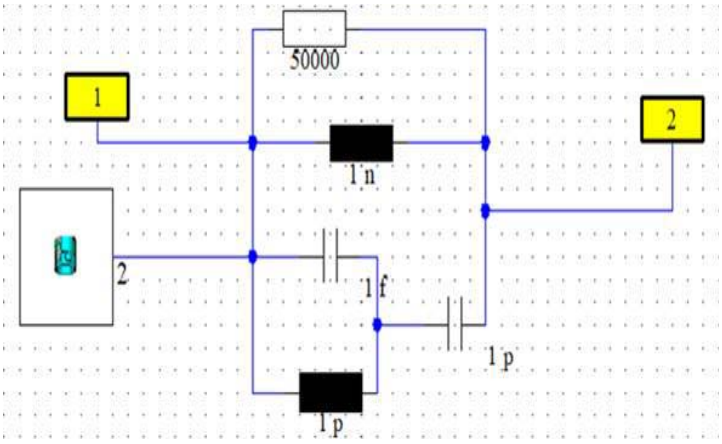

Figure 6. Matching circuit configuration.

structure on a cylindrical profile. The matching circuit is shown in Fig. 6.

For the bending configuration, CST MW based on FIT formulation is performed for the proposed antenna structure with a resolution of 1 mm to characterize the antenna performance in terms of resonant frequency, bandwidth, gain, and radiation efficiency. The proposed antenna spectra $|S_{11}|$ based on two switch cases bending configuration are shown in Fig. 7. It is noticed that the frequency is shifted to 5.03 GHz which is related to antenna bending.

The authors presented the phase difference of the proposed folded antenna structure (see Fig. 8), to ensure the antenna performance at the same reliability when bent. The phase difference about 173.22° is considered to be negligible.

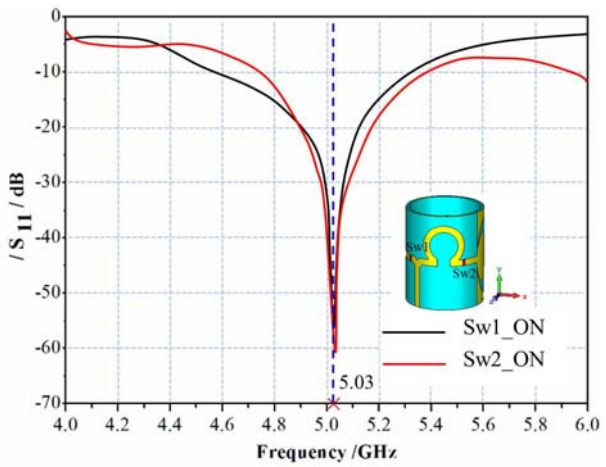

Figure 7. $|S_{11}|$ Spectra of the proposed antenna at two switch cases based on folded profile.

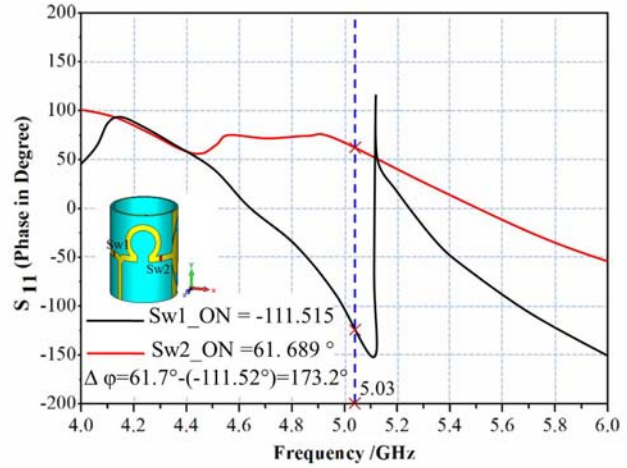

Figure 8. $|S_{11}|$ Spectra of the proposed antenna at two switches cases based on folded profile.

4.4. Comparison between the Planar and Folded Antenna Profiles

The planar and folded antenna profile performances are investigated in this section in terms of $|S_{11}|$, gain, bandwidth, phase-difference, and radiation pattern. From the simulated results (see Figs. 7 and 8), it is found that the folded antenna profile exhibits a shift in the frequency resonance from 5 GHz to 5.03 GHz. The frequency shift is attributed to the effects of patch bending that realizes surface current motion on a substrate [12]. The impedance matching is improved for the folded profile, and simultaneously, the realized gain is reduced without significant effects on antenna bandwidth compared

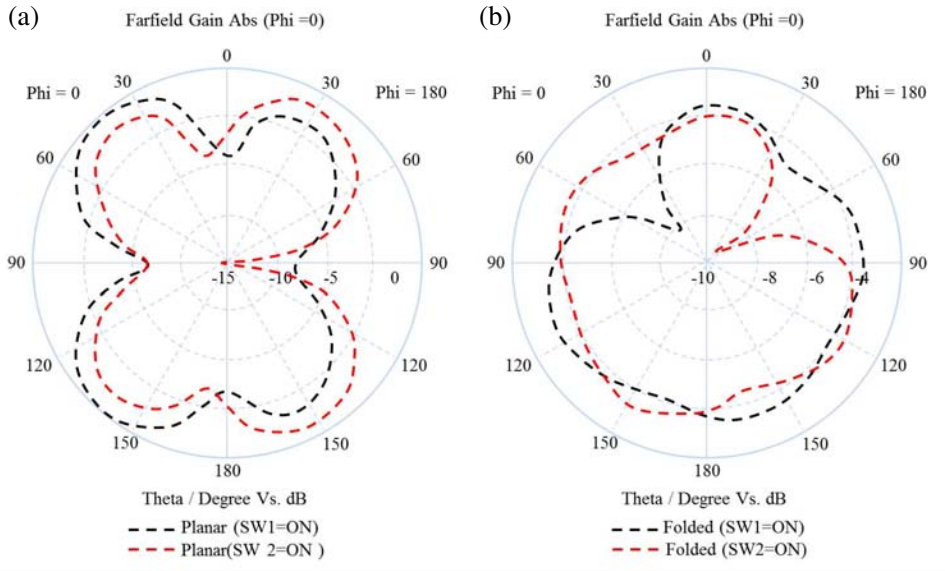

Figure 9. The *E*-plane radiation patterns for (a) planar and (b) folded antenna profile.

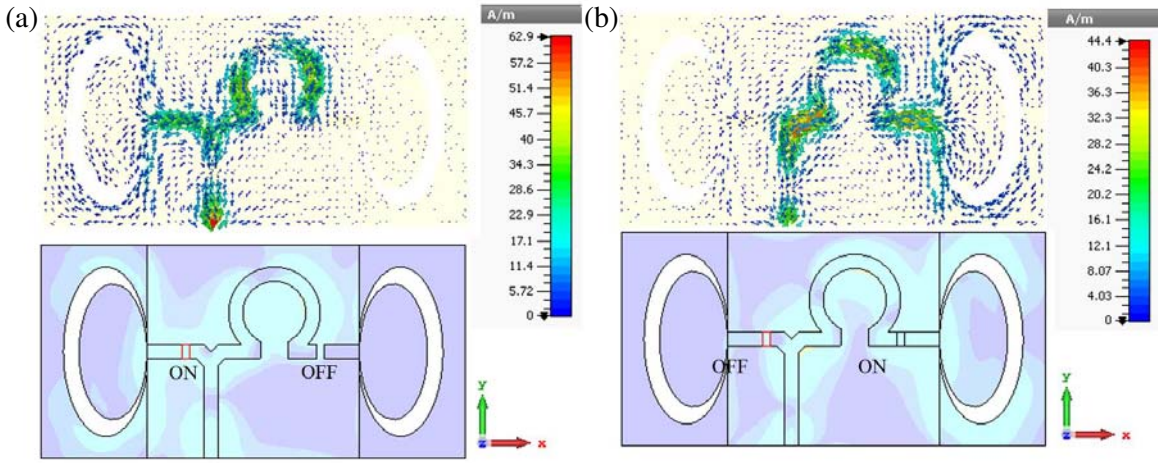

Figure 10. The current distribution of the proposed antenna at 5 GHz when (a) SW1 is ON, and SW2 is OFF and (b) SW1 is OFF, and SW2 is ON.

to the planar profile as seen in Figs. 4, 5, 7, and 8. Furthermore, the phase difference between the antenna patches for the folded profile is unaffected compared to the planar antenna profile. A slight reduction in the antenna gain is taken place for the folded profile due to the back lobe increase after bending [39]. The folded profile antenna pattern is changed due to the entire antenna surface current change, where the energy mostly radiates in the forward direction. Furthermore, as seen in Fig. 9, the radiation pattern from the folded antenna disperses to different directions that severely affects the antenna gain and efficiency.

Based on the two switches scenarios, the surface-current distributions of the proposed planar antenna configuration are shown in Fig. 10 at 5 GHz. It is found that when the SW1 is OFF, the current moves toward the second patch; however, by switching SW2 OFF the current moves back toward the first patch.

The gain pattern for the two switches scenarios is calculated and plotted in 3D-form at 5 GHz as shown in Fig. 11. The gain is evaluated from CST MWS. It is found that the realized gain is equal to 4.15 dB when the SW1 is ON and SW2 OFF, and by switching SW1 OFF and SW2 ON, the gain is

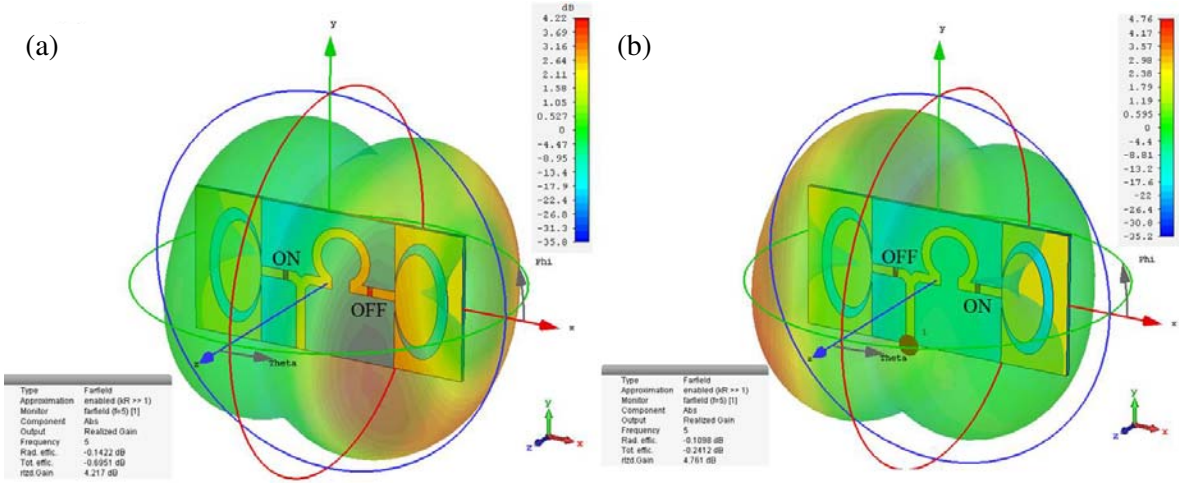

Figure 11. 3D radiation patterns of the proposed antenna at 5 GHz when (a) SW1 is ON, and SW2 is OFF and (b) SW1 is OFF, and SW2 is ON.

changed to 4.73 dB.

The comparison of the proposed antenna performances based on the planar and folded profiles is shown in Table 2. As indicated from Table 2, the planar profile shows comparatively more gain-bandwidth product than the folded profile as expected. The folded antenna profile provides enhanced impedance.

Table 2. Comparison between planar and folded antenna performance.

Antenna profile	Frequency (GHz)	$\|S_{11}\|$ (dBi)	Bandwidth (MHz)	Gain (dB)	Phase
Planar (SW1-ON)	5	−10.55	334	4.15	173.2°
Planar (SW2-ON)	5	−12.6	1190	4.73	−7.4°
Folded (SW1-ON)	5.03	−55	752	2.45	−111.6°
Folded (SW2-ON)	5.03	−62	646	2.50	61.7°

5. RESULTS VALIDATION AND MEASUREMENTS

After applying the numerical study to arrive at the optimal antenna design, the authors attempted to fabricate the proposed antenna based on the planar configuration, as shown in Fig. 12. The proposed antenna is fabricated in the laboratory of printed wiring boards of BME-ETT in the Department of Electronic Technology (ETT) of Budapest University of Technology and Economics (BME). A Printed Circuit Board (PCB) technique is used to fabricate the proposed antenna on a Roger RO3203 substrate. The fabricated antenna is fed through a 50 Ω RF SMA connector, as seen in Fig. 12. The SMA connector is welded to the transmission line of the patch antenna. Two PIN diodes of BAR6303W high-speed switching RF signals are used as switching elements. The two PIN diodes are soldered with a heating soldering technique to avoid damages due to the direct high-temperature contact. Using two pairs of cables for the PIN diodes (ON-OFF) state, an RF choke is used in series with a biased thread needed to provide a DC supply to the PIN diode cathode and to prevent the RF from flowing into the DC supply. A bias tee adapter is used to connect the antenna to the RF source.

The measured and simulated performances in terms of $|S_{11}|$ spectra of the planar profile around the design frequency band are presented in Fig. 13. As shown in Fig. 13, the obtained simulated and measured results show an acceptable agreement. It is found that if PIN diode 1 (SW1) is ON and PIN diode 2 (SW2) OFF, the $|S_{11}| < -10$ dB is equal to −10.55 dB at 5 GHz for the simulated results while it

Figure 12. The fabricated antenna with PIN diodes; (a) front view, (b) back view and (c) biasing the PIN diode.

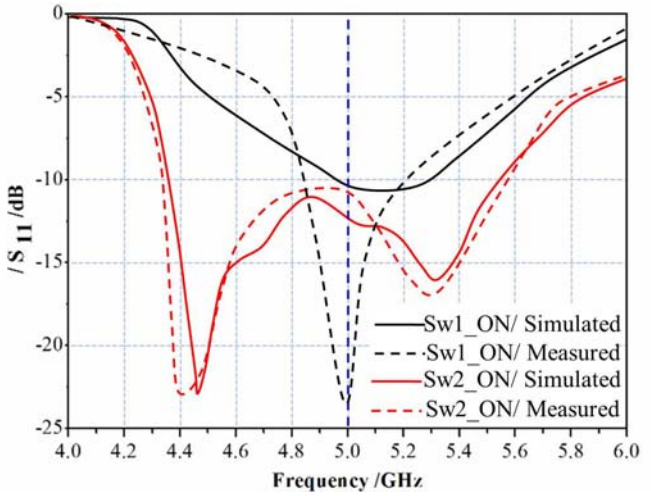

Figure 13. Simulated and measured $|S_{11}|$ spectra of the proposed antenna at two cases based on planar profile.

is equal to −23.8 dB for the measured results at 5 GHz. On the other hand, it is found that if PIN diode 2 (SW2) is ON and PIN diode 1 (SW1) OFF, the $|S_{11}| < -10$ dB is equal to −12.6 dB for the simulated results and equal to −10.94 dB for the measured results at 5 GHz. A slight discrepancy between the simulated and measured results is found due to the technical accuracy for the modeling of the antenna system, making it challenging to obtain the similarity between the measured and simulated results for both states. The experimental measurements are tested using Vector Network Analyzer STAR ms4642A Series and inside an RF anechoic chamber.

The simulated and measured far-field radiation patterns for the proposed antenna based on the two PIN diode states are shown in Fig. 14. It is observed that a good agreement between the measured and simulated results has been obtained for the two PIN diodes states. The CST MW simulation does not include the parasitic effects; therefore, the pattern changes are expected for conformal configurations since not full matching and a slight shift in antenna radiation is made between the measured and simulated results as depicted in Fig. 14. For this, the antenna gain and radiation patterns are measured inside an RF chamber using a three-antenna method. The process is basically realized by conducting a standard dipole antenna at the frequency band of interest after calibrating the path losses inside the chamber.

The simulated and measured results of the proposed planar antenna performances are summarized and listed in Table 3 for detailed comparisons. A good agreement has been obtained between the simulated and measured results, as shown in Table 3.

6. ANTENNA PERFORMANCE-BASED WEARABLE APPLICATIONS

In order to use the proposed antenna for wearable applications, bending or crumpling of the proposed

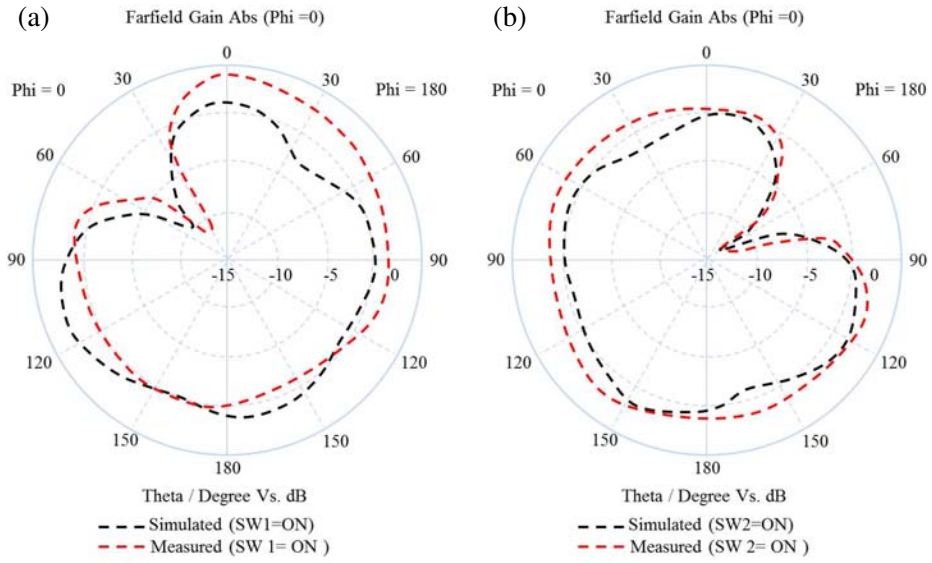

Figure 14. Simulated and measured radiation patterns for the proposed antenna.

Table 3. The simulated and measured performance of the proposed antenna based on planar profile.

Simulated/Measured	Switch status	Frequency (GHz)	$\|S_{11}\|$ (dB)	Bandwidth (MHz)	Gain (dBi)
Simulated	SW1 (ON), SW2 (OFF)	5	−10.55	334	4.15
Simulated	SW1 (OFF), SW2 (ON)	5	−12.6	1190	4.73
Measured	SW1 (ON), SW2 (OFF)	5	−23.8	356	4.07
Measured	SW1 (OFF), SW2 (ON)	5	−10.94	1245	4.55

antenna when being mounted on human body could be a subject of the mechanical effects on the antenna. A numerical study is applied to the proposed antenna to be bent with different radii to ensure this purpose suitability. The proposed antenna is examined with four different radii: 20 mm, 40 mm, 60 mm, and 80 mm; these radii are considered due to the possible varying of the human arms and legs sizes. The proposed planar antennas under different bending conditions are illustrated in Fig. 15.

Figure 16 shows the proposed antenna performances in terms of S_{11} and gain spectra for two switching cases, based on different bending radii. It influences the resonant frequency, which is shifted to a lower frequency band with increasing the bending effect. A slight impedance reduction occurred when the bending increased beyond 80 mm. In general, the antenna bandwidth is found to be affected significantly due to the bending effect for both switching cases.

Figure 17 shows the simulated 2D radiation patterns based on two switching cases, with different radius deformation in the E-plane and H-plane. Table 4 summarizes the proposed antenna performances based on different radii values.

The antenna performance on the human body is discussed in this section when the proposed antenna is mounted on the biological tissues. Hence, different hazards could be associated with the fields fringing from such antennas [40]. To meet such wearable antenna requirements, the Specific Absorption Rate (SAR) for the bent antenna structure is examined on the human body. SAR measurement is an industrial standard that signifies the amount of energy absorbed by the biological tissues [41]. The proposed bent antenna effect on the human body is numerically tested using CSTMW. The evaluation is conducted on the human hand model. For the proposed scenario, the folded antenna is mounted around the human hand by modeling the analysis with four layers of tissues: skin, fat, muscle, and bone. The average

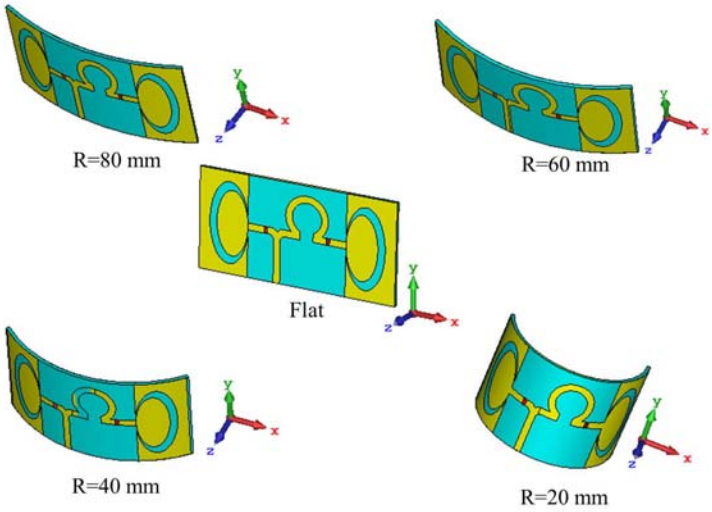

Figure 15. Structural deformation of the proposed antenna, with different radius curvature values.

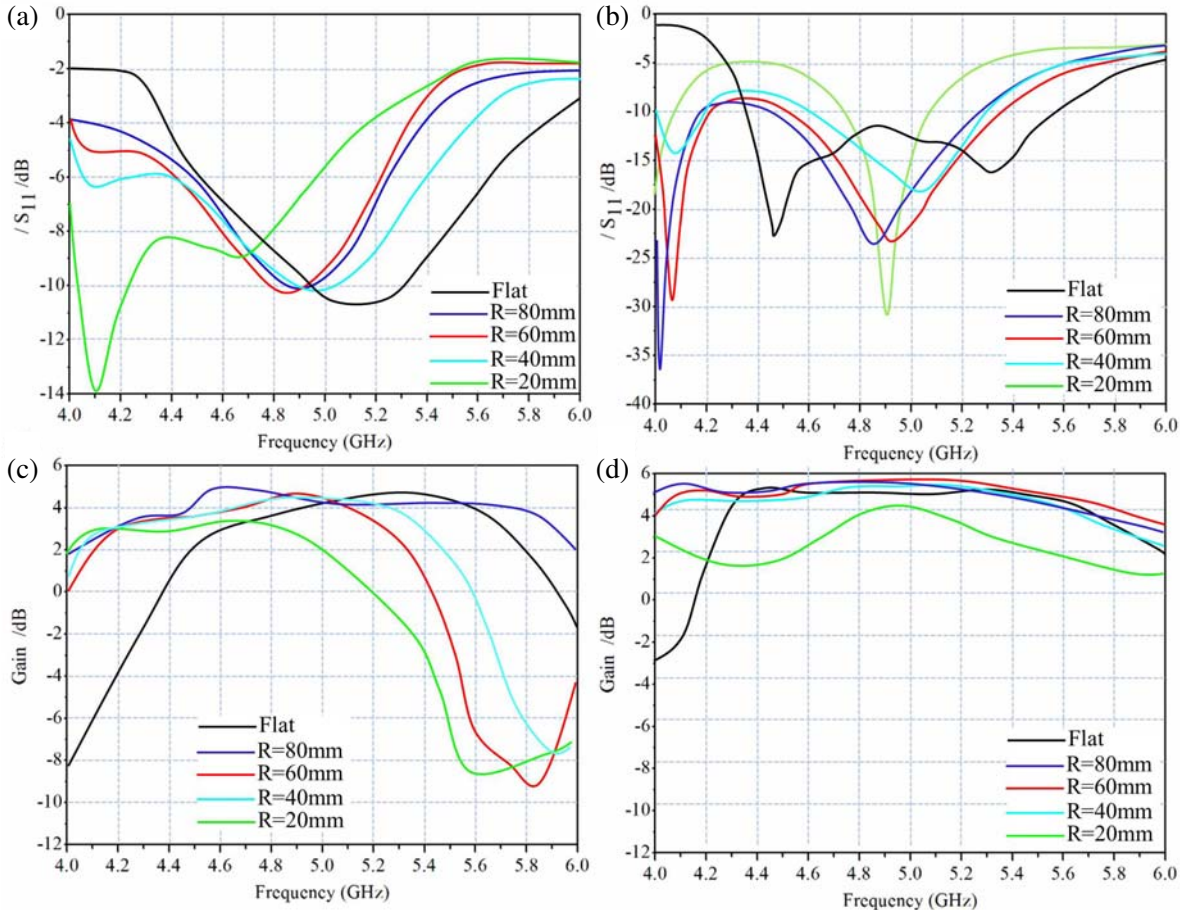

Figure 16. Simulated S_{11} for (a) SW1 (ON), SW2 (OFF) and (b) for SW1 (OFF), SW2 (ON), gain for (c) SW1 (ON), SW2 (OFF) and (d) for SW1 (OFF), SW2 (ON) with different values of the curvature radius.

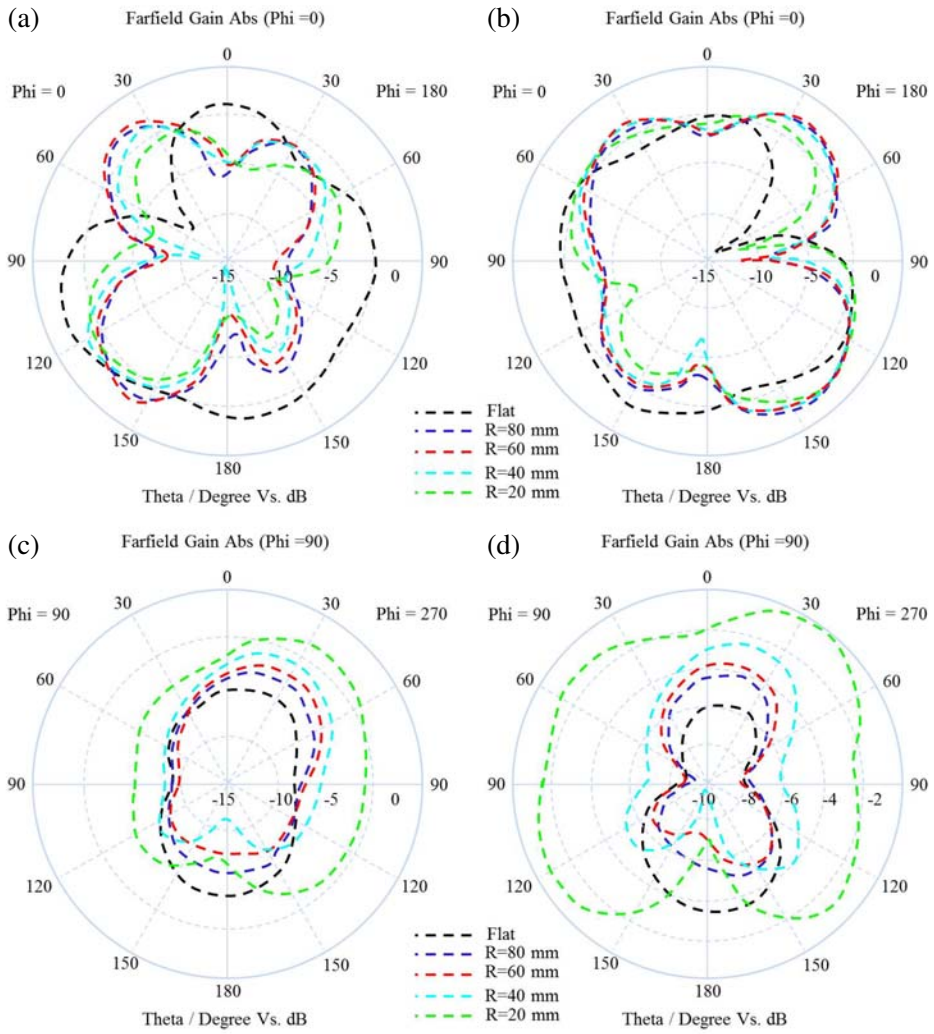

Figure 17. The simulated radiation pattern for the proposed antenna in (a) E-plane and (c) H-plane when SW1 (ON), SW2 (OFF), and (b) E-plane and (d) H-plane when SW1 (OFF), SW2 (ON) with different radius values of deformation.

intrinsic properties of these tissues are described in Table 5, valid at 5 GHz [42]. The authors chose the skin dry, bone-cortical values for numerical simulation to simulate the human hand mode. The proposed antenna should offer appropriate radiation characteristics with low SAR at 5 GHz, and the SAR threshold should be below 2 W/kg [43]. For calculating the SAR value, the formulation given in Equation (2) [43] can be used. CSTMW is utilized to evaluate the proposed antenna performance when the proposed antenna is formed as a planar rectangular, bent structure and cylindrical frame in touch with the human arm, head, and chest, separately. As shown in Fig. 17, such cases are modeled as a nonhomogeneous layer. The size of the flat antenna profile is considered as 30 mm × 60 mm. The radius is fixed to 45 mm for the bent configuration, and for the folded configuration it is set to 9.5 mm. All the proposed models are shown in Fig. 18 with a summary of the human body tissues properties at 5 GHz in Table 5. The SAR is calculated using the following equation:

$$SAR = \frac{\sigma |E^2|}{\rho} \tag{2}$$

where σ is the electrical conductivity, E the electrical field, and ρ the density.

As far as S_{11} spectra of the proposed antenna are concerned, an analogous response for various curvature profiles is obtained and presented in Fig. 19. The resonant frequencies for the two bending

Table 4. The simulated performance of the proposed antenna under different radii values.

R (mm)	Switch status	Frequency (GHz)	$\|S_{11}\|$ (dB)	Bandwidth (MHz)	Gain (dBi)	Efficiency %
Flat	(SW1-ON, SW2-OFF)	5	−10.55	334	4.15	97.1
Flat	(SW1-OFF, SW2-ON)	5	−12.6	1190	4.73	97.1
80	(SW1-ON, SW2-OFF)	4.87	−10.8	150	5.17	97.6
80	(SW1-OFF, SW2-ON)	4.88	−23.5	800	5.15	97.7
60	(SW1-ON, SW2-OFF)	4.87	−10.2	185	4.73	97
60	(SW1-OFF, SW2-ON)	4.95	−23	850	5.35	97.7
40	(SW1-ON, SW2-OFF)	4.96	−10.5	200	5.78	97.3
40	(SW1-OFF, SW2-ON)	5.06	−18	700	5.23	97.7
20	(SW1-ON, SW2-OFF)	4.12	−14	210	3.5	94.6
20	(SW1-OFF, SW2-ON)	4.92	−31	313	4.15	96.5

Table 5. Properties of human body tissues [32].

Tissue	Relative permittivity (ϵ_r)	Conductivity (σ) S/m	Density (Kg/m^3)	Loss tangent ($\tan\delta$)	Thickness (mm)
Skin Wet	39.611	3.5744	1100	0.32441	0.3
Skin Dry	35.774	3.0608	1100	0.3076	0.3
Fat	5.0291	0.2422	1100	0.17315	3
Muscle	49.54	4.0448	1060	0.29353	2.1
Bone Cancellous	70.774	0.12282	1850	0.0579	3.3
Bone Cortical	36.772	0.042822	1850	0.34459	3.3
Bone Marrow	19.269	0.0110905	1850	0.16683	3.3

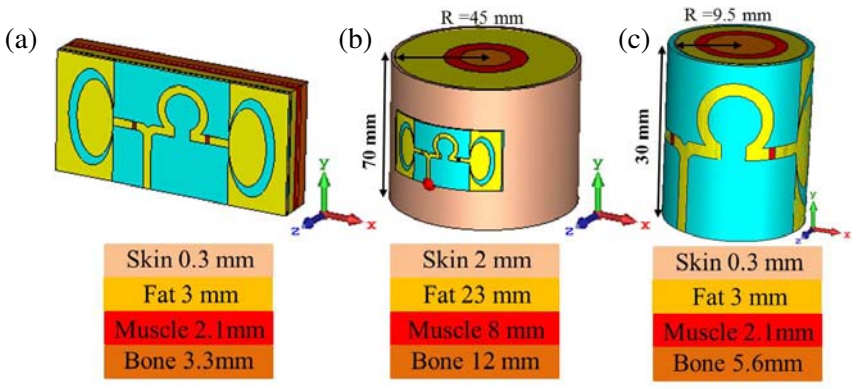

Figure 18. The layout of the proposed antennas (a) mounted on human tissue, (b) bent around a human arm, and (c) surrounded the human hand.

configurations are found almost the same as for the planar structure. Based on these deformations, a slight change in the S_{11} matching value and resonant frequency is found for the two switching cases, as seen in Fig. 19. However, the folded structure does not show a significant change in the resonant frequency for the proposed antenna, while severe frequency change has occurred in the case of bending.

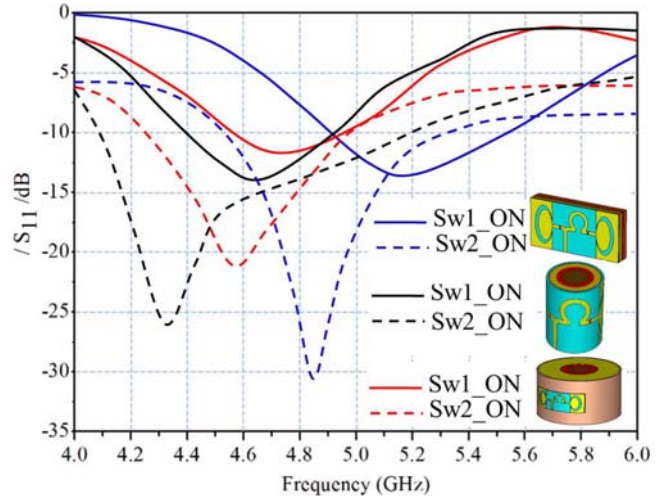

Figure 19. Comparison of simulated S_{11} spectra of the proposed antenna based on a human tissue under three conditions.

The main reason for this is the patch current surface change when the proposed antenna is shaped as cylindrical geometry [44]. For the aspect of switching effects, the flat structure S_{11} matching impedance is found about -14 dB at 5.15 GHz when SW1 is (ON) and SW2 (ON), S_{11} is found -31.5 dB at 4.85 GHz. As expected, more shift in operating frequency occurs in the case of the folded and bent profiles. S_{11} for the bent profile is found to be -14 dB at 4.65 GHz when SW1 is switched (ON), while when SW2 is switched (ON), S_{11} is changed to -26.5 dB at 4.34 GHz. The S_{11} for the folded antenna profile is changed to -11.8 dB at 4.58 GHz when SW1 is (ON) and is changed to -21.5 dB at 4.5 GHz when SW2 is (ON). Table 6 shows more details about the effects of switching scenarios on the antenna performance in planar, bent, and folded profiles.

Table 6. Comparisons of the proposed antenna performance based on planar, bent, and folded profile.

Antenna Type	Frequency (GHz)	S_{11} (dB)	Gain (dBi)	Bandwidth (MHz)	Phase shift (degree)
Planar (SW1-ON, SW2-OFF)	5.15	-14	4.15	612	173.2°
Planar (SW1-OFF, SW2-ON)	4.85	-31.5	4.73	775	-7.4°
Bent (SW1-ON, SW2-OFF)	4.65	-14	4.7	375	132.6°
Bent (SW1-OFF, SW2-ON)	4.34	-26.5	4.82	675	-41.9°
Folded (SW1-ON, SW2-OFF)	4.58	-11.8	2.45	525	-111.6°
Folded (SW1-OFF, SW2-ON)	4.5	-21.5	2.5	1125	61.7°

The absorbed radiation effects on the human body are studied experimentally by monitoring the absorption quantity in a given scenarios on the human arm, head, thigh, and chest. It is observed from the listed results in Table 7 that the proposed antenna array shows minimum radiation leakage when being bent over the arm. It is found that the field strength leakage from the antenna toward the arm is about 47 mV/m. However, the field strength is increased rapidly on the chest for the flat case up to 207 mV/m. The reason is that the arm size is mostly leasing compared to other human parts that absorb less radiation [40]. These measurements are performed by placing the TM-195 RF 3-axis field strength meter at 10 mm away from the human body but on the other side from the antenna back. Table 7 shows a comparison between the field strength leakages at different scenarios from the human body parts.

Table 7. Comparison between the field strength leakage at different scenarios from the human body parts.

Location	Profile	Field strength (mV/m)
Arm	Planar	50
Arm	Bended	47
Head	Planar	199
Head	Bended	188
Thigh	Planar	140
Thigh	Bended	150
Chest	Planar	207
Chest	Bended	189

Table 8. Comparison between the proposed antenna performances with the published works.

Reference	Profile	Frequency (GHz)	Dimension $(mm)^2$	Gain (dBi)	Reconfiguration	Application
[16]	Planar	1.4	114×88	N	Frequency, Polarization	Satellite navigation
[18]	Planar	2.45, 3, 3.69, 5.5	15×40	2.92	Frequency	Bluetooth, WLAN, WiMAX, LTE
[19]	Planar	8.88	N	N	Beam steering	Radar, Radio
[20]	Planar	0.85, 0.9, 1.8, 1.9, 2.1, 0.7, 2.3	65×114	2.92	Frequency	Bluetooth, WLAN, WiMAX, LTE
[21]	Planar	4.97, 4.77, 6.78	15.5×16.4	5.5–6.5	Polarization	WLAN, Wi-Fi
[22]	Planar	2.42, 2.36, 3.36	31×59	N	Frequency, Polarization	WLAN, WiMAX
[23]	Planar	1.95, 2.14	50×75	N	BPSK modulation	Modulation
[24]	Planar	N	45×20	N	Pattern	QPSK
[25]	Planar	0.85–1.45	22×225	4.5–6.5	Bandwidth, Pattern	N
[27]	Planar	UWB	32×26	2.5	Band-notch	Cognitive radio
[28]	Planar	UWB	20×20	0–3	Pulse modulation	N
[29]	Planar	UWB	805×90	1–2	Frequency	IR/UWB, WLAN, WiMAX
[30]	Planar	3.1, 6.8	23×31	4.01, 4.6	Frequency, Pattern	N
[32]	Planar	UWB	25×35	2–5	Band-notch	WiMax, WLAN
[35]	Planar	1.8	112.5×283.5	2.3	Frequency	8-PSK, IoT
[45]	Planar	UWB	30×60	4.5	N	IoT
Proposed	Planar, Folded	5	30×60	4.73, 2.5	Phase Modulation	DPSK

To highlight the viability of the proposed antenna design, this work is compared with the previously published results regarding antenna profile, size, gain and type of the antenna reconfigurable. Table 8 shows the performances of the proposed antenna compared with other published work, it is indicated that the novelty of the proposed work is represented by designing antenna to work within two profiles, planar and folded unlike other published work, the antenna design work within only planar profile. And the proposed direct modulation embedded with the antenna structure which makes the proposed antenna a good candidate for many wearable and implantable wireless applications. The simplicity of controlling the the proposed antenna modulation is another achieved in this work, making the design, fabrication, and test the proposed antenna simple compared with other published work.

7. CONCLUSION

For DAM based on spread spectrum technology, a simple planar and folded antenna profile is presented in this article. The proposed antenna is mounted on a flexible substrate for wearable applications. The proposed antenna consists of two patches with the same geometry for DPSK process. The patch structure is fed with a 50 Ω microstrip line network of two branches and delayed by a phase shift of 180° at different frequencies. The phase shift is controlled based on two PIN diodes. The proposed antenna performance on the human body based on planar, bent and folded profiles is investigated. The proposed antenna is examined based on a human tissue under three scenarios with four layers: skin, fat, muscle, and bone tissues. Since the proposed antenna is designed for biomedical applications, the biological effects from exposure to electromagnetic radiation of the human body are investigated in this paper. The field strength from the proposed antenna array is measured at different human body locations with different scenarios using a 3D axis field strength meter. The proposed antenna is found to be a good candidate for multiple wireless communications systems in particular, the wearable applications. Compared to other related work, the novelty of the proposed work is the simplicity of controlling the switching mechanism, as an excellent candidate for wearable systems. The proposed antenna structure, compared to earlier reported works, is in low profile, simple, easy to fabricate, easy to control the phase shifting and activation of the antenna, and easy to integrate with other devices. As a future work for this research, the authors are willing to adapt the antenna performance with varying the gain value to quadrature amplitude-shift keying modulation.

ACKNOWLEDGMENT

The research reported in this paper and carried out at the BME has been supported by the NRDI Fund based on the charter of bolster issued by the NRDI Office under the auspices of the Ministry for Innovation and Technology. The author Yahiea Al Naiemy would like to record his indebtedness to the Tempus Public Foundation Stipendium Hungaricum program and the University of Diyala-Iraq for their support for his Ph.D. scholarship.

REFERENCES

1. Glover, I. and P. M. Grant, *Digital Communications*, Pearson Education, 2010.
2. Henthorn, S., K. L. Ford, and T. O'Farrell, "Bit-error-rate performance of quadrature modulation transmission using reconfigurable frequency selective surfaces," *IEEE Antennas and Wireless Propagation Letters*, Vol. 16, 2038–2041, 2017.
3. Babakhani, A., D. B. Rutledge, and A. Hajimiri, "Transmitter architectures based on near-field direct antenna modulation," *IEEE Journal of Solid-State Circuits*, Vol. 43, No. 12, 2674–2692, 2008.
4. Mohamadzade, B., R. B. Simorangkir, S. Maric, A. Lalbakhsh, K. P. Esselle, and R. M. Hashmi, "Recent developments and state of the art in flexible and conformal reconfigurable antennas," *Electronics*, Vol. 9, No. 9, 1375, 2020.

5. Bernhard, J. T., "Reconfigurable antennas," *Synthesis Lectures on Antennas*, Vol. 2, No. 1, 1–66, 2007.
6. Christodoulou, C. G., Y. Tawk, S. A. Lane, and S. R. Erwin, "Reconfigurable antennas for wireless and space applications," *Proceedings of the IEEE*, Vol. 100, No. 7, 2250–2261, 2012.
7. Eldek, A., A. Abdallah, and M. Manzoul, "Reconfigurable microstrip double-dipole antennas for personal wireless communications," *Wireless Engineering and Technology*, Vol. 2, No. 2, 60–69, 2011.
8. Matin, M. A., "Recent trends in antennas for modern wireless communications," *Wearable Technologies: Concepts, Methodologies, Tools, and Applications*, 1413–1435, IGI Global, 2018.
9. Dahlman, E., Y. Jading, S. Parkvall, and H. Murai, "3G radio access evolution — HSPA and LTE for mobile broadband —," *IEICE Transactions on Communications*, Vol. 92, No. 5, 1432–1440, 2009.
10. Yashchyshyn, Y., "Reconfigurable antennas by RF switches technology," *2009 5th International Conference on Perspective Technologies and Methods in MEMS Design*, 155–157, IEEE, 2009.
11. Al Naiemy, Y., T. A. Elwi, and L. Nagy, "An end fire printed monopole antenna based on electromagnetic band gap structure," *Automatika*, Vol. 61, No. 3, 482–495, 2020.
12. Alnaiemy, Y, T. A. Elwi, and L. Nagy, "Mutual coupling reduction in patch antenna array based on EBG structure for MIMO applications," *Periodica Polytechnica Electrical Engineering and Computer Science*, Vol. 63, No. 4, 332–342, 2019.
13. AlSabbagh, H. M., T. A. Elwi, Y. Al-Naiemy, and H. M. Al-Rizzo, "A compact triple-band metamaterial-inspired antenna for wearable applications," *Microwave and Optical Technology Letters*, Vol. 62, No. 2, 763–777, 2020.
14. Alnaiemy, Y., T. A. Elwi, L. Nagy, and T. Zwick, "A systematic analysis and design of a high gain microstrip antenna based on a single EBG layer," 2019.
15. Hassain, Z. A., A. R. Azeez, M. M. Ali, and T. A. Elwi, "A modified compact Bi-directional UWB taperd slot antenna with double band-notch characteristics," *Advanced Electromagnetics*, Vol. 8, No. 4, 74–79, 2019.
16. Wang, H., Z. Wu, Y. Wang, C.-Y.-D. Sim, and G. Yang, "Small-size folded monopole antenna with switchable matching circuit for ultra-thin mobile applications," *Progress In Electromagnetics Research C*, Vol. 65, 131–138, 2016.
17. Elwi, T. A., "Electromagnetic band gap structures based on ultra wideband microstrip antenna," *Microwave and Optical Technology Letters*, Vol. 59, No. 4, 827–834, 2017.
18. Liang, B., B. Sanz-Izquierdo, E. A. Parker, and J. C. Batchelor, "A frequency and polarization reconfigurable circularly polarized antenna using active EBG structure for satellite navigation," *IEEE Transactions on Antennas and Propagation*, Vol. 63, No. 1, 33–40, 2014.
19. Singh, D. K., B. K. Kanaujia, S. Dwari, G. P. Pandey, and S. Kumar, "Reconfigurable circularly polarized capacitive coupled microstrip antenna," *International Journal of Microwave and Wireless Technologies*, Vol. 9, No. 4, 843, 2017.
20. Saeed, S. M., C. A. Balanis, and C. R. Birtcher, "Inkjet-printed flexible reconfigurable antenna for conformal WLAN/WiMAX wireless devices," *IEEE Antennas and Wireless Propagation Letters*, Vol. 15, 1979–1982, 2016.
21. Yousefbeiki, M. and J. Perruisseau-Carrier, "Towards compact and frequency-tunable antenna solutions for MIMO transmission with a single RF chain," *IEEE Transactions on Antennas and Propagation*, Vol. 62, No. 3, 1065–1073, 2013.
22. Yousefbeiki, M., O. N. Alrabadi, and J. Perruisseau-Carrier, "Efficient MIMO transmission of PSK signals with a single-radio reconfigurable antenna," *IEEE Transactions on Communications*, Vol. 62, No. 2, 567–577, 2014.
23. Pringle, L. N., P. H. Harms, S. P. Blalock, G. N. Kiesel, E. J. Kuster, P. G. Friederich, R. J. Prado, J. M. Morris, and G. S. Smith, "A reconfigurable aperture antenna based on switched links between electrically small metallic patches," *IEEE Transactions on Antennas and Propagation*, Vol. 52, No. 6, 1434–1445, 2004.

24. Chia, M.-W., T.-H. Lim, J.-K. Yin, P.-Y. Chee, S.-W. Leong, and C.-K. Sim, "Electronic beam-steering design for UWB phased array," *IEEE Transactions on Microwave Theory and Techniques*, Vol. 54, No. 6, 2431–2438, 2006.
25. Yin, Z., Q. Zheng, K. Guo, and Z. Guo, "Tunable beam steering, focusing and generating of orbital angular momentum vortex beams using high-order patch array," *Applied Sciences*, Vol. 9, No. 15, 2949, 2019.
26. Yao, W. and Y. E. Wang, "An integrated antenna for pulse modulation and radiation," *Proceedings 2004 IEEE Radio and Wireless Conference (IEEE Cat. No. 04TH8746)*, 427–429, IEEE, 2004.
27. Mohammed, A. A., F. M. Alnahwi, A. S. Abdullah, and A. G. A. A. Hameed, "A compact monopole antenna with reconfigurable band notch for underlay cognitive radio applications," *2018 International Conference on Advance of Sustainable Engineering and Its Application (ICASEA)*, 25–30, IEEE, 2018.
28. Tasouji, N., J. Nourinia, C. Ghobadi, and F. Tofigh, "A novel printed UWB slot antenna with reconfigurable band-notch characteristics," *IEEE Antennas and Wireless Propagation Letters*, Vol. 12, 922–925, 2013.
29. Zhang, Z. and Z. Pan, "Time domain performance of reconfigurable filter antenna for IR-UWB, WLAN, and WiMAX applications," *Electronics*, Vol. 8, No. 9, 1007, 2019.
30. Iqbal, A., A. Smida, N. K. Mallat, R. Ghayoula, I. Elfergani, J. Rodriguez, and S. Kim, "Frequency and pattern reconfigurable antenna for emerging wireless communication systems," *Electronics*, Vol. 8, No. 4, 407, 2019.
31. Ojaroudi Parchin, N., H. Jahanbakhsh Basherlou, Y. I. Al-Yasir, R. A. Abd-Alhameed, A. M. Abdulkhaleq, and J. M. Noras, "Recent developments of reconfigurable antennas for current and future wireless communication systems," *Electronics*, Vol. 8, No. 2, 128, 2019.
32. Yang, H., X. Xi, H. Hou, X. Shi, and Y. Yuan, "Design of reconfigurable monopole antenna with switchable dual band-notches for UWB applications," *International Journal of Microwave and Wireless Technologies*, Vol. 10, No. 9, 1065–1071, 2018.
33. Manteghi, M., "A wideband electrically small transient-state antenna," *IEEE Transactions on Antennas and Propagation*, Vol. 64, No. 4, 1201–1208, 2016.
34. Kiani, G. I. and T. S. Bird, "ASK modulator based on switchable FSS for THz applications," *Radio Science*, Vol. 46, No. 02, 1–8, 2011.
35. Henthorn, S., K. L. Ford, and T. O'Farrell, "Direct antenna modulation for high-order phase shift keying," *IEEE Transactions on Antennas and Propagation*, Vol. 68, No. 1, 111–120, 2019.
36. Srivastava, S. and J. J. Adams, "Analysis of a direct antenna modulation transmitter for wideband OOK with a narrowband antenna," *IEEE Transactions on Antennas and Propagation*, Vol. 65, No. 10, 4971–4979, 2017.
37. Tang, W., J. Y. Dai, M. Chen, X. Li, Q. Cheng, S. Jin, K.-K. Wong, and T. J. Cui, "Programmable metasurface-based rf chain-free 8PSK wireless transmitter," *Electronics Letters*, Vol. 55, No. 7, 417–420, 2019.
38. Diaby, F., A. Clemente, L. Di Palma, L. Dussopt, K. Pham, E. Fourn, and R. Sauleau, "Linearlypolarized electronically reconfigurable transmitarray antenna with 2-bit phase resolution in Ka-band," *2017 International Conference on Electromagnetics in Advanced Applications (ICEAA)*, 1295–1298, IEEE, 2017.
39. Alnaiemy, Y., T. A. Elwi, and N. Lajos, "A folded microstrip antenna structure based differential phase shift keying modulation technique," *2018 IEEE 18th International Symposium on Computational Intelligence and Informatics (CINTI)*, 000 071–000 074, IEEE, 2018.
40. Il Kwak, S., D.-U. Sim, J. H. Kwon, and Y. J. Yoon, "Design of PIFA with metamaterials for body-SAR reduction in wearable applications," *IEEE Transactions on Electromagnetic Compatibility*, Vol. 59, No. 1, 297–300, 2016.
41. Ahmed, H. S. and T. A. Elwi, "SAR effect reduction using reject band filter arrays for Wi-Fi portable devices," *International Journal of Electronics Letters*, Vol. 7, No. 2, 236–248, 2019.

42. Andreuccetti, D., R. Fossi, and C. Petrucc, "Dielectric properties of body tissues: HTML clients," *IFACCNR*, Vol. 2007, Florence, Italy, 1997.
43. Ali, U., S. Ullah, M. Shafi, S. A. Shah, I. A. Shah, and J. A. Flint, "Design and comparative analysis of conventional and metamaterial-based textile antennas for wearable applications," *International Journal of Numerical Modelling: Electronic Networks, Devices and Fields*, Vol. 32, No. 6, e2567, 2019.
44. Elwi, T. A. and A. M. Al-Saegh, "Further realization of a flexible metamaterial-based antenna on indium nickel oxide polymerized palm fiber substrates for RF energy harvesting," *International Journal of Microwave and Wireless Technologies*, 1–9, 2020.
45. Elwi, T. A., O. A. Tawfeeq, Y. Alnaiemy, H. S. Ahmed, and N. Lajos, "A UWB monopole antenna design based RF energy harvesting technology," *2018 Third Scientific Conference of Electrical Engineering (SCEE)*, 111–115, IEEE, 2018.